How Variable are Cold Pools?

Leah D. Grant[1*], Bastian Kirsch[2,3*], Jennie Bukowski[1], Nicholas M. Falk[1], Christine A. Neumaier[1], Mirjana Sakradzija[3,4], Susan C. van den Heever[1], and Felix Ament[2,3]

[1] Department of Atmospheric Science, Colorado State University, Fort Collins, CO, United States.

[2] Meteorological Institute, University of Hamburg, Hamburg, Germany.

[3] Hans Ertel Centre for Weather Research, Germany.

[4] Deutscher Wetterdienst, Offenbach am Main, Germany.

[*]These authors have contributed equally.

Corresponding authors: Leah D. Grant (leah.grant@colostate.edu) and Bastian Kirsch (bastian.kirsch@uni-hamburg.de)

Key Points:

- Cold pool impacts on sub-mesoscale temperature variability are quantified using variograms derived from observations and simulations.
- Cold pools enhance temperature variability on scales between 5 and 15 km, but the magnitude varies strongly with lifetime and environment.
- High-resolution case-study and idealized simulations underestimate the magnitude of cold pool variability, irrespective of resolution.

Abstract

Cold pools formed by precipitating convective clouds are an important source of mesoscale temperature variability. However, their sub-mesoscale (100 m to 10 km) structure has not been studied, which impedes validation of numerical models and understanding of their atmospheric and societal impacts. We quantify temperature variability in observed and simulated cold pools using variograms calculated from dense network observations collected during a field experiment and in high-resolution case study and idealized simulations. The temperature variance in cold pools is enhanced for spatial scales between ~5-15 km compared to pre-cold pool conditions, but the magnitude varies strongly with cold pool evolution and environment. Simulations capture the overall cold pool variogram shape well but underestimate the magnitude of the variability, irrespective of model resolution. Temperature variograms outside of cold pool periods are represented by the range of simulations evaluated here, suggesting that models misrepresent cold pool formation and/or dissipation processes.

Plain Language Summary

Cold pools are cool gusty winds beneath thunderstorms that are formed by cooling from rainfall. They have many important impacts in the atmosphere and on society but are difficult to properly simulate in numerical weather models. The variability in cold pool temperature is an understudied feature of cold pools but which is important to represent in numerical models. In this study, we examine cold pool temperature variability from a dense network of surface weather station observations collected during a field campaign, and we compare those observations to numerical simulations of cold pools in a range of environments. We find that cold pools enhance temperature variability for distances greater than ~5 km but suppress variability on smaller distances, and that the magnitude of cold pool temperature variability is strongly dependent on the environment and cold pool lifetime. We also show that numerical models, even at very high resolutions, are not able to properly simulate the magnitude of cold pool temperature variability. We highlight areas for improvement in numerical models that may help to improve simulations of cold pool variability, including land-atmosphere interactions, turbulence, and conversion processes between water vapor and condensed water in storms.

1 Introduction

Cold pools, regions of dense air formed by precipitation that propagate as density currents (Byers and Braham, 1949; Benjamin, 1968), are ubiquitous atmospheric phenomena that can occur with any type of precipitating cloud. They also play a myriad of important roles in weather, climate, and society: they initiate convection and influence convective system properties (e.g. Purdom, 1976; Wilson & Schreiber, 1986; Rotunno et al., 1988; Khairoutdinov & Randall, 2006; Schlemmer & Hohenegger, 2014), loft aerosols such as dust and biological particles (Marks et al., 2001; Bou Karam et al., 2009; Seigel & van den Heever, 2012; Bukowski & van den Heever, 2022), and impact aviation operations (Fujita, 1978). In images of laboratory density currents or dust-lofting atmospheric cold pools called haboobs (e.g. see Simpson, 1969, Fig. 1, Fig. 7), multi-scale turbulent structures are evident, implying that cold pool properties should exhibit variability on scales ranging from meters to the size of the cold pool itself. And

yet, little is known about the magnitude or structure of this variability from observations and numerical simulations. Understanding this variability is crucial to assessing cold pool representation in large-eddy simulation (LES), numerical weather prediction, and climate models, and to understanding their many atmospheric and societal impacts.

Simulated cold pool properties, and how they interact with other components of the earth system, are known to be sensitive to the model grid spacing, as shown in previous modeling studies (Straka et al., 1993; Bryan et al., 2003; Grant & van den Heever, 2016; Huang et al., 2018; Hirt et al., 2020; Fiévet et al., 2023). Many of these studies have demonstrated more intense, longer-lived, and faster-propagating cold pools at finer model resolutions. Droegemeier and Wilhelmson (1987) and Straka et al. (1993) showed that turbulent structures in cold pools are not appropriately represented until 100 m or finer grid spacings are used. Grant and van den Heever (2016) further recommended horizontal (vertical) grid spacings of 100 m (50 m) or finer to simulate not only the impacts of turbulent structures on the cold pool properties, but also to accurately capture cold pool interactions with the land surface. Hirt et al. (2020) showed that coarser resolutions directly lead to weaker upward mass flux at cold pool edges, with impacts on convective initiation.

Far fewer studies have investigated the variability in individual cold pools within observations, largely due to limited spatial resolutions of traditional observing networks. Two recent observational campaigns have been conducted to address this gap. van den Heever et al. (2021) used a *flying curtain* strategy to measure cold pools on scales of 100 m to 1 km in the High Plains of the U.S. They found variations in temperature and wind on scales of 1 km and finer. Dense networks of surface meteorological stations in Germany observed temperature gradients inside a cold pool of up to 9 K / 7 km (Kirsch et al., 2022b; Hohenegger et al., 2023).

As evidenced by this previous work, scale interactions in cold pools are critical to their properties, lifetimes, interactions with earth's surface and convection, and societal impacts. Yet, comprehensive analyses of the scales of variability in observed cold pools have not been performed, nor have these scales been assessed in numerical models. In this study we aim to fill this important knowledge gap by addressing the following questions, with a focus on cold pool *temperature* as a critical component of cold pool density and hence its first-order properties:

(1) What are the scales of temperature variability within observed cold pools?

(2) How accurately do numerical models, with grid spacings of order 100 m to 1 km, represent this observed variability?

(3) What is the sensitivity of cold pool temperature variability to environmental conditions?

We investigate these questions using novel observations from a recent field campaign, the Field Experiment on Submesoscale Spatio-Temporal Variability in Lindenberg (FESSTVaL; Hohenegger et al., 2023), designed to measure fine spatio-temporal variability in cold pool properties. We also directly assess the ability of numerical models to accurately represent this variability as a function of model resolution and environment, using case study simulations of observed cold pool events during FESSTVaL as well as case study and idealized simulations of

cold pools in a range of other environments. We find that models generally do *not* accurately represent observed variability in cold pool temperatures, even at LES grid spacings, and highlight key areas for improvement in simulating processes contributing to cold pool properties and lifetimes.

2 Methods

2.1 FESSTVaL observations

The observational data set used in this study was collected during the FESSTVaL field experiment held in eastern Germany from 17 May to 27 August 2021 (Hohenegger et al., 2023). During FESSTVaL, 42 cold pool events were observed (Kirsch et al., 2023a). The air temperature data were recorded by 99 custom-built, low-cost measurement stations (Kirsch et al., 2022b), which were arranged as a dense network covering a 30 km-diameter circular area centered at the Lindenberg observatory. Nearest-neighbor distances ranged from 100 m to 4.8 km (Fig. 1a; Fig. S1; Kirsch et al., 2023a). The network design allows for an examination of variability within individual cold pools on scales from 100 m to 15 km. All raw sub-minute temperature data are smoothed with a 1-min running average filter. On 29 June 2021, a cold pool named "Jogi" was observed by the network (Fig. 1a). Jogi was the strongest cold pool event of the campaign, initiating at around 1530 local time (LT) and lasting for ~2 hours (Fig. S2), and is analyzed in detail in this study.

2.2 Quantifying spatial variability

We quantify the spatial variability of the near-surface air temperature field using variograms (Chils & Delfiner, 1999; Wackernagel, 2003). The variogram analysis is a tool often used in geostatistics to characterize the spatial heterogeneity of a regionalized, stochastic variable. The underlying variogram function of a given variable (temperature T in this case) that is sampled at selected locations can be estimated from its empirical variogram ($\hat{\gamma}$). $\hat{\gamma}$ is calculated by forming pairs of sample locations $i \neq j$ and binning them according to their distances d (Fig. 1a). The variogram function for distance bin d, with $N(d)$ samples, is given by:

$$\hat{\gamma}(d) = \frac{1}{2}\frac{1}{N(d)}\sum_{i \neq j}\left(T_j - T_i\right)^2 \qquad \text{(Eq. 1)}$$

As a trade-off between resolution and statistical stability, we choose a 500 m bin width to calculate all empirical variograms in this study (Fig. S1). The maximum variogram distance corresponds to half the domain size (15 km; Wackernagel, 2003). Variograms are calculated for observed FESSTVaL data and in the simulation data by superimposing the network on the model grid and linearly interpolating the model data at the lowest level above ground to the station locations.

140 2.3 Simulations

141 A collection of simulation sets is analyzed to examine simulated cold pool variability in a
142 range of environments and model resolutions. These include case study simulations of cold pool
143 Jogi and a tropical maritime cold pool, and three sets of idealized cold pool simulations in dry
144 continental conditions with varying background environments. All simulation names, grid
145 spacings, output frequencies, FESSTVaL network placements, and cold pool lifetimes are
146 summarized in Table S1, while the cold pool properties for one simulation in each set are
147 summarized in Table 1.

148 Table 1. *Names and Cold Pool Properties for OBS-Jogi and Select Simulations*

Name	T_{ref} (°C) [a]	ΔT_{mean}, ΔT_{min} (K) [b]	σ_{mean}, σ_{max} (K) [b]
OBS-Jogi	28.6	-2.7, -11.5	2.51, 3.40
CS-Jogi-156m	29.0	-0.8, -9.5	1.07, 2.04
CS-TropOce-100m	27.3	-1.6, -4.4	0.69, 1.05
IDEAL-DryBL-50m	28.5	-1.0, -9.7	1.27, 3.28
IDEAL-DownShear-100m	20.9	-6.6, -15.6	1.61, 4.62
IDEAL-UpShear-100m	20.9	-3.7, -16.8	3.05, 4.95
IDEAL-Haboob-20KDay-150m	43.28	-1.15, -15.77	1.62, 6.24

149 Note: Simulations are named beginning with IDEAL (for idealized) or CS (for case study),
150 followed by a brief description of the environment, followed by the horizontal grid spacing. [a]T_{ref}:
151 Mean temperature across all stations and over 1-h period before cold pool onset. [b]ΔT_{mean}, ΔT_{min},
152 σ_{mean}, σ_{max}: Mean temperature (T) or standard deviation (σ) across all stations and over 1-h
153 period after cold pool onset, or minimum/maximum across all stations and cold pool lifetime.

154

155 **CS-Jogi simulations:** Case study simulations for cold pool Jogi are performed using the
156 Icosahedral Nonhydrostatic model in LES mode (ICON-LES; Dipankar et al., 2015; Text S1).
157 The modeling setup consists of four elliptical domains with grid spacings of 625 m, 312 m, 156
158 m (see Fig. 1b), and 75 m, centered around the FESSTVaL experiment area in eastern Germany.
159 Note that the maximum diameter of the CS-Jogi-75m simulation domain is 24 km and, therefore,
160 smaller than the FESSTVaL network. Thus, variograms are only shown up to 10 km (Fig. S1).

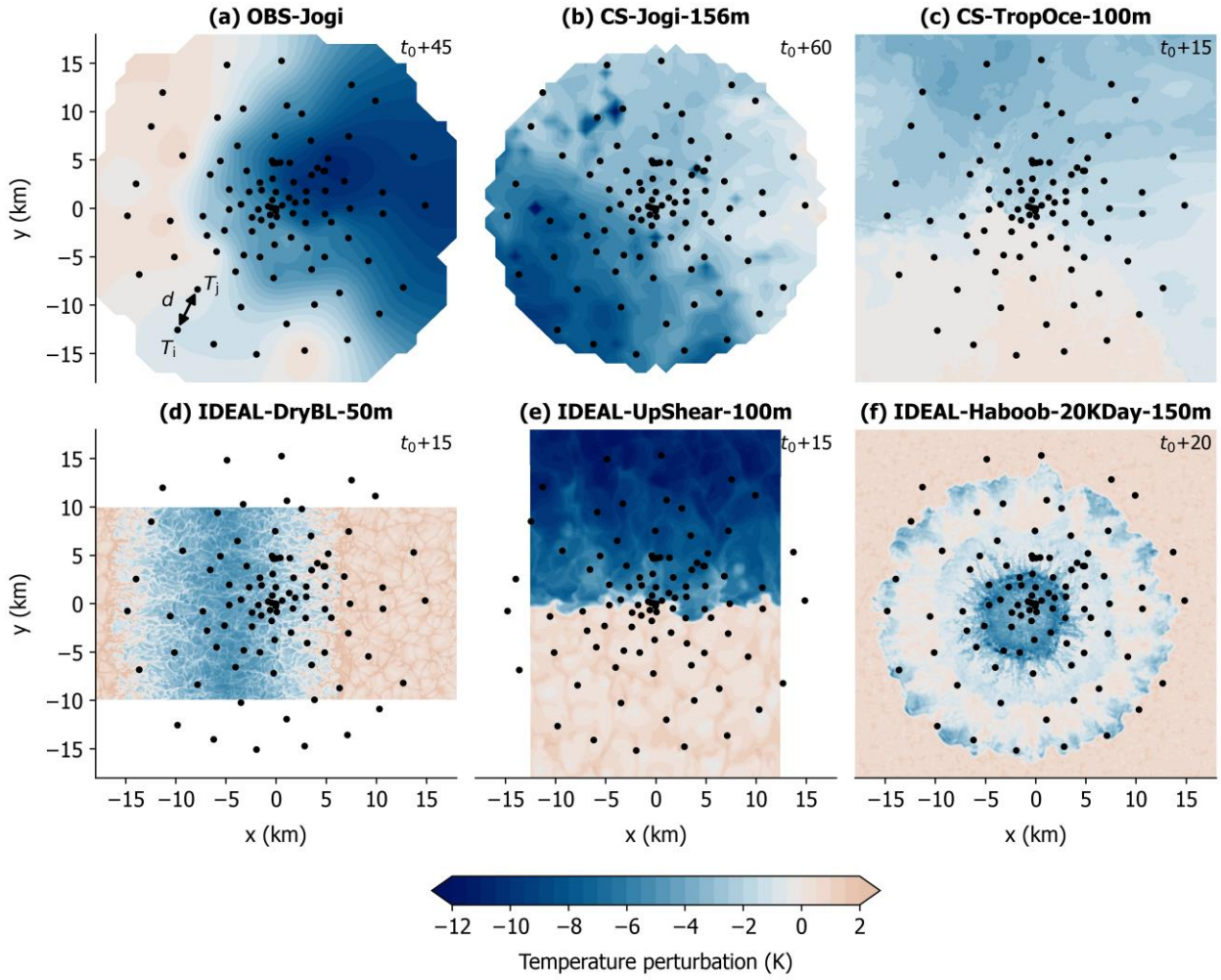

Figure 1. Plan views of temperature perturbations relative to the reference temperature (Table 1) for (a) observations from the Jogi case (spatially interpolated for better visualization), (b) a Jogi case study simulation, and (c-f) other case study and idealized simulations. Model data are shown at the lowest level above ground. In each panel, time (min) since cold pool onset (t_0) is labeled at the top right and the FESSTVaL network is overlain in black dots. Coordinates are relative to the network center. Notations in (a) refer to quantities shown in Eq. (1).

CS-TropOce simulations: Case study simulations with 1 km horizontal grid spacing are performed using the Regional Atmospheric Modeling System (RAMS; Cotton et al., 2003; Saleeby & van den Heever, 2013) for the NASA Cloud, Aerosol, and Monsoon Processes Philippines Experiment (CAMP^{2}Ex; Reid et al., 2023, S.3.2). A cold pool that occurred west of Luzon is included in our analysis (simulation CS-TropOce-1km; Text S1). A higher resolution simulation (CS-TropOce-100m; Text S1) is also conducted (Fig. 1c).

IDEAL-DryBL simulations: An idealized LES of a linear cold pool dissipating by surface fluxes and entrainment in a deep, turbulent boundary layer is conducted with RAMS (IDEAL-DryBL-50m, Fig. 1d; Grant & van den Heever, 2018a). The initial land surface and

atmospheric conditions are horizontally homogeneous, and there is no background wind shear, interactions with clouds, nor microphysical processes. A coarser simulation (IDEAL-DryBL-100m) is also included.

IDEAL-Shear simulations: These simulations conducted using RAMS are similar to the IDEAL-DryBL simulations, except that the environment includes ~20 m s^{-1} vertical wind shear over the lowest 3 km, and the x-direction is a narrow channel (Text S1). Simulations with two different horizontal grid spacings are included (IDEAL-Shear-100m (Fig. 1e) and IDEAL-Shear-250m). In both simulations, two networks are imposed: one downshear and one upshear, hereafter called the IDEAL-DownShear and IDEAL-UpShear (Fig. 1e) simulations, respectively. The background wind speed limits the upshear cold pool propagation while increasing the downshear leading edge propagation speed.

IDEAL-Haboob-150m simulations: Bukowski and van den Heever (2022) describe a 120-simulation ensemble of idealized dust-producing cold pools (haboobs) in an arid, desert-like environment using RAMS, a single circular cold bubble approach, and no background winds or microphysical processes. For this study, eight simulations are subset from the ensemble: four each during daytime and nighttime with initial cold pool temperature deficits ranging from 10 to 20 K (Fig. 1f; for more details see Section 3.3).

3 Results

3.1 Observed temperature variability

To address our first science question, *What are the scales of temperature variability within observed cold pools?*, we first examine the variogram for the 42 cold pools observed throughout the 103-day period of the FESSTVaL campaign (Fig. 2a). As a baseline reference, we also analyze the variogram for all daytime non-cold pool events. On average, cold pools enhance temperature variance on spatial scales between 5-15 km. As previous studies have shown, cold pools tend to be at least 5 km in diameter (Kirsch et al. 2022b, 2023a; Terai & Wood, 2013; Feng et al., 2015) and introduce footprints in the temperature field on the scale of the cold pool itself. These footprints are larger in spatial scale than temperature variations caused by boundary layer processes such as Rayleigh-Benard convection (Lord Rayleigh, 1916), which tend to scale with the depth of the boundary layer (e.g. Hardy & Ottersten, 1969). Interestingly, Fig. 2a also indicates that on average, cold pools reduce temperature variance on spatial scales less than ~4 km. This may indicate mechanical mixing by the enhanced winds within relative to outside the cold pool. Additionally, cold pools are stably stratified and may, on average, suppress surface sensible heat fluxes, thus reducing surface-driven turbulence, although previous studies have suggested sensible heat fluxes can be enhanced within cold pools under certain conditions (Grant & van den Heever, 2016, 2018a; Gentine et al., 2016; Bukowski & van den Heever, 2021). Finally, it is instructive to note the different shapes of the cold pool and non-cold pool variograms. The daytime non-cold pool variogram slope is steeper at small scales but flattens out at scales above ~5 km, which indicates that the dominant scales of variability due to boundary layer motions are 5 km and smaller. However, the cold pool variogram slope is more linear across the range of scales.

We next examine the variogram results for the Jogi case (OBS-Jogi; Fig. 2b). While most cold pools from the FESSTVaL record (31) had median temperature deficits of 4 K or weaker (Kirsch et al., 2023a), the Jogi cold pool had a maximum temperature deficit of 11.5 K (Table 1). This is in line with previous observations of strong cold pools (e.g. Engerer et al., 2008; Kirsch et al., 2021; van den Heever et al., 2021). The OBS-Jogi temperature variogram is almost an order of magnitude larger than the average variograms for other observed cold pools (Fig. 2b). This indicates that the strongest cold pools can have exceptionally high magnitude variograms compared to cold pools overall, and that the relative enhancement in temperature variance for strong cold pools is greater than the relative enhancement in mean cold pool strength.

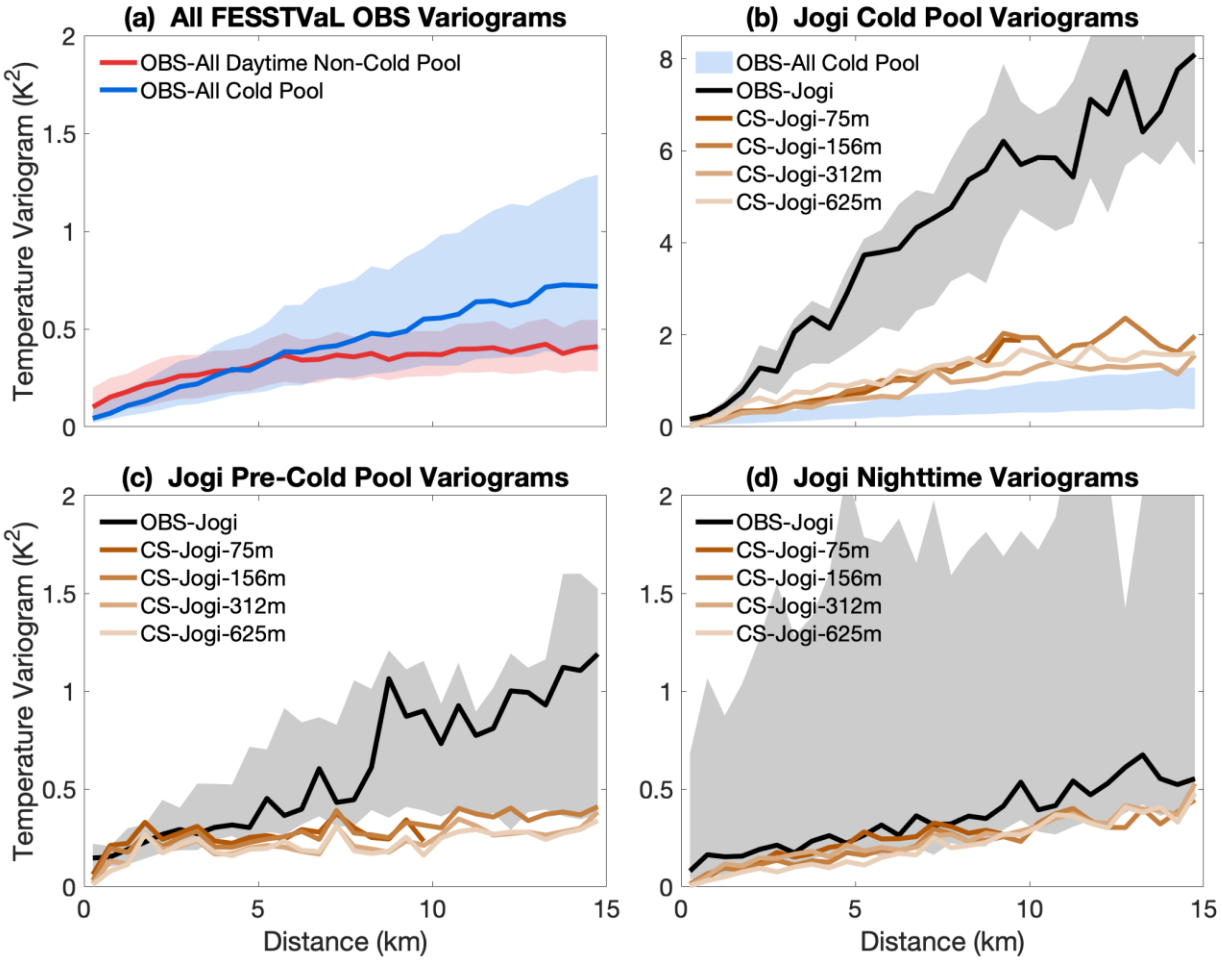

Fig. 2. (a) Temperature variograms during cold pool (2 h after onset) and daytime (11-18 LT) non-cold time periods every 15 min for the entire duration of the FESSTVaL dataset. (b) Comparison between all observed cold pools (blue shading, same as in panel (a)), the OBS-Jogi case every 1 min, and the CS-Jogi simulations as labeled in the legend. Note the different y-axis scale compared to the other panels. (c) Variograms for 3-h periods before cold pool onset for Jogi observations and simulations. (d) As in (c) but over nighttime periods (22-05 LT). All solid lines (shading) represent the median (interquartile range).

3.2 Comparing observed and simulated temperature variability

We address our second question, *How accurately do numerical models represent the observed temperature variability?*, by directly comparing the CS-Jogi case study simulations to the observations (Fig. 2b). While the temperature variogram in the simulated Jogi cold pools have the correct shape, they are not strong enough, with their median magnitude being ~1/3 that seen in the observations and outside the OBS-Jogi interquartile range. Remarkably, the model resolution does not make a large difference to the simulated temperature variance. Nevertheless, all four CS-Jogi simulations well approximate the mean cold pool temperature deficit and its temporal evolution (Fig. 1a-b; Fig. S2). In fact, the simulations have an even stronger mean temperature deficit than seen in the observations (Fig. S2), although the maximum deficit at any one station and the standard deviations across the network are larger in the observations (Table 1). Overall, this result demonstrates that temperature variance is not properly represented even when the mean cold pool properties are well-simulated.

To assess reasons for the simulation's misrepresentation of the observed cold pool temperature variance, we examine variograms in the pre-cold pool (Fig. 2c) and nocturnal boundary layer (Fig. 2d). Pre-cold pool variograms are well-simulated at small scales, but underestimated at scales above ~5 km (Fig. 2c). The larger-scale variance underestimation stems from a small pre-Jogi cold pool in the observations which isn't present in the simulations (not shown). The agreement below 5 km indicates that the scales of variability induced by boundary layer circulations are well-represented in the simulations. Second, the nighttime variogram magnitudes in the CS-Jogi simulations are slightly underestimated but within the OBS-Jogi interquartile range (Fig. 2d). At night when the boundary layer stabilizes, temperature variance is primarily driven by topographic-driven differences in station elevations across the FESSTVaL network. The agreement between the nighttime CS-Jogi and OBS-Jogi data indicates the topography is also well-resolved in the simulations, consistent with the fine spatial resolution of the ICON-LES input topography data (Text S1). In summary, the non-cold pool variogram comparisons suggest that the model underestimation of cold pool temperature variability is *not* due to misrepresentation of boundary layer circulations, surface heterogeneity, or topography. Rather, it likely results from poor simulation of processes contributing to internal cold pool variability, like spatial variations in evaporative cooling rates, turbulence mixing, and responding surface fluxes within the cold pool.

3.3 Sensitivity of cold pool variability to environment and model resolution

In this section, we examine the sensitivity of cold pool temperature variability to the cold pool's environmental conditions and to model resolution to further answer our second question and address our third question, *What is the sensitivity of cold pool temperature variability to environmental conditions?*. Fig. 3a-b summarize the impacts of the environment on cold pool temperature variability. The environment has a very strong control on cold pool temperature variance. Cold pools forming in contrasting environments, such as tropical maritime versus midlatitude continental cold pools, can have more than an order of magnitude difference in temperature variograms (compare CS-TropOce-100m to IDEAL-UpShear-100m; Fig. 3a, Fig.

1c,e). Tropical maritime cold pools are typically much weaker than midlatitude continental ones (Table 1, Fig. 1, Zuidema et al., 2012; van den Heever et al., 2021; Simoes-Sousa et al., 2022) and to first order, one might expect weaker cold pools to exhibit smaller variability. The IDEAL-Haboob ensemble, in which the initial cold pool temperature deficit was varied, confirms this point (Fig. 3b): initially stronger cold pools have larger temperature variance, all else equal. Second, cold pool temperature variance can be vastly different even in the same background environment, as evidenced by the variogram differences between the upshear and downshear sides of the cold pool in the IDEAL-Shear simulations arising from different residence times in the network (Fig. 3a). Third, the IDEAL-Haboob ensemble (Fig. 3b) shows that all else equal, nocturnal cold pools have larger temperature variability than during the day, and nighttime cold pool variability is more sensitive to the cold pool strength than during the daytime. Daytime cold pools dissipate faster than the nighttime ones due to surface sensible heating and mixing with the turbulent boundary layer (Bukowski & van den Heever, 2022), thus demonstrating the important control of cold pool dissipation processes on temperature variability.

Fig. 3a reconfirms the results from the CS-Jogi simulation set (Fig. 2b): remarkably, resolution does not strongly impact simulated cold pool temperature variability, counter to what we might expect based on prior literature showing more intense cold pools with finer resolution (see section 1). The largest difference in variogram magnitude with increasing resolution is seen in the IDEAL-DryBL simulation set, which has the highest resolution overall and is the only LES set in which the vertical grid spacing is also varied, both of which may enhance the change in variogram magnitude.

In the simulations and observations (Fig. 3c), there is large temporal variability in cold pool temperature variance, with the greatest magnitudes seen near cold pool onset. However, the variogram magnitude drops off quickly toward the pre-cold pool values in most simulations, especially in continental cold pools undergoing fast dissipation processes (e.g. IDEAL-DryBL-50m, IDEAL-Shear-100m, and IDEAL-Haboob). This again underscores the importance of processes influencing cold pool lifetimes in contributing to the magnitude and evolution of cold pool variability. Finally, while some simulations exhibit peak variogram magnitudes equal to or exceeding the peak for OBS-Jogi, none come close to the OBS-Jogi median variogram magnitude (compare Fig. 2b with Fig. 3a-b), despite the fact that some of the simulated cold pools have similar or even larger temperature deficits than OBS-Jogi (e.g. IDEAL-Shear-100m; Table 1). Thus, even when mean cold pool properties are similar to (or stronger than) observed, simulated cold pool temperature variability is still not properly represented at LES resolutions.

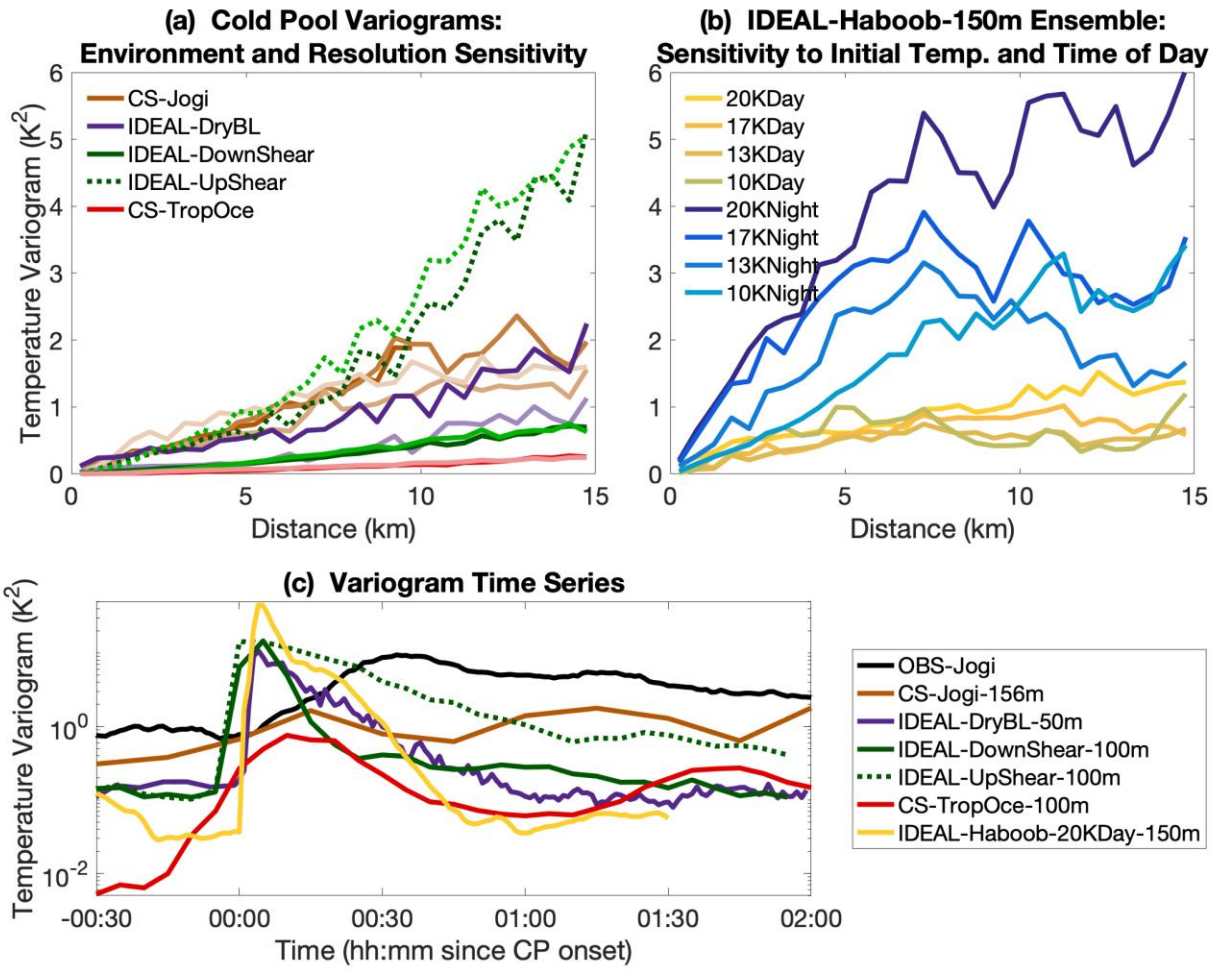

Figure 3. (a) As in Fig. 2b, but comparing the impact of environment and model grid spacing on median variogram magnitudes. Darker colors indicate higher resolution simulations. (b) Median variograms for the IDEAL-Haboob-150m ensemble, showing variation in variogram magnitudes as a function of initial cold pool temperature and day (yellow lines) versus night (blue lines). (c) Time series of median variogram magnitude across all bins for OBS-Jogi and select simulations as labeled in the legend. Note the log y-axis scaling.

4 Conclusions

In this study we have investigated the footprints of cold pools on temperature variability, their representation in numerical models, and their sensitivity to environmental conditions using novel fine-spatio-temporal resolution measurements from the FESSTVaL field campaign, case study simulations of a FESSTVaL cold pool event, and a collection of case study and idealized simulations. This is an essential research topic not investigated previously but needed to better understand cold pool processes, their interactions with convection and earth's surface, and their societal impacts. Variograms are an effective tool to characterize the temperature variability and can be applied equally well to model simulations and dense station network observations, thereby enabling easy and fair comparisons. We investigated three science questions which are summarized below:

1. *What are the scales of temperature variability within observed cold pools?* The FESSTVaL observations show that cold pools enhance spatial temperature variability on scales greater than ~5 km, but suppress variability on smaller scales, likely by mechanical mixing of boundary layer circulations. The magnitude of cold pool temperature variability is highly temporally variable and greatly enhanced for stronger cold pools.

2. *How accurately do numerical models, with grid spacings of order 100 m to 1 km, represent this observed variability?* By comparing an observed cold pool with case study simulations of the same event, we find that numerical models substantially underestimate the observed cold pool temperature variability, even when the mean cold pool properties are well represented. Finer resolution does not significantly improve model representation of cold pool variability.

3. What is the sensitivity of cold pool temperature variability to environmental conditions? The suite of simulations examined in this study demonstrate strong sensitivity of the variability to environmental conditions. Tropical maritime cold pools are less variable than midlatitude continental ones. Cold pool variability is also sensitive to background wind shear, time of day, and the cold pool strength, with stronger cold pools exhibiting larger variability.

Our analysis of pre-cold pool and nighttime temperature variance in non-cold pool conditions along with the evolution of cold pool temperature variability lead us to conclude that models likely underestimate the magnitude of cold pool temperature variability due to misrepresentation of physical processes contributing to cold pool lifetimes, namely, latent cooling stemming from microphysical processes and dissipation by entrainment and surface fluxes. These are critical areas for future investigation and improvement in numerical models if we are to improve predictions of cold pools and their many important implications for weather, climate, and society.

Acknowledgments

Funding was provided by HErZ of DWD and the German Federal Ministry of Transport and Digital Infrastructure and by the German Research Foundation DFG under Germany‘s Excellence Strategy, EXC 2037 CLICCS, Project 390683824, by the National Science Foundation grants AGS-2029611, AGS-2105938, and AGS-2019947, and by the National Aeronautics and Space Administration grant 80NSSC18K0149.

LDG and BK have contributed equally to this work.

Availability Statement

All scripts and NetCDF files containing variogram and model output data used to create figures and table information in this manuscript and in the supporting information are available on GitHub via https://doi.org/10.5281/zenodo.8433896 (Kirsch et al., 2023b).

The APOLLO and WXT observational data sets of FESSTVaL 2021 are available from Universität Hamburg via https://doi.org/10.25592/UHHFDM.10179 (Kirsch et al., 2022a).

Model output and/or source code for each set of simulations used in the analyses is available from the following sources:

- CS-Jogi simulations: Zenodo via https://doi.org/10.5281/zenodo.8411098 (Sakradzija, 2023). See also the FESSTVaL final report at https://fesstval.de/fileadmin/user_upload/fesstval/Files/FESSTVaL-Report-final.pdf (accessed 2023-10-09) (accessed 2023-10-09)
- CS-TropOce simulations: GitHub via https://doi.org/10.5281/zenodo.8411499 (Falk et al., 2023).
- IDEAL-DryBL simulations: Mountain Scholar via https://doi.org/10.25675/10217/186403 (Grant & van den Heever, 2018b).
- IDEAL-Shear simulations: GitHub via https://doi.org/10.5281/zenodo.8411979 (Neumaier et al., 2023).
- IDEAL-Haboob-150m ensemble: Dryad via https://doi:10.5061/dryad.6hdr7sr4d (Bukowski & van den Heever, 2023).

References

Benjamin, T. B. (1968). Gravity currents and related phenomena. Journal of Fluid Mechanics, 31(02), 209–248. doi:10.1017/S0022112068000133

Bou Karam, D., Williams, E., Janiga, M., Flamant, C., McGraw-Herdeg, M., Cuesta, J., Auby, A., & Thorncroft, C. (2014). Synoptic-scale dust emissions over the Sahara Desert initiated by a moist convective cold pool in early August 2006. *Quart. J. Roy. Meteor. Soc.*, 140, 2591–2607. doi:10.1002/qj.2326

Bryan, G. H., Wyngaard, J. C., & Fritsch, J. M. (2003). Resolution requirements for the simulation of deep moist convection. *Monthly Weather Review*, 131(10), 2394–2416. https://doi.org/10.1175/1520-0493(2003)131<2394:rrftso>2.0.co;2

Bukowski, J., & van den Heever, S. C. (2021). Direct radiative effects in haboobs. *J. Geophys. Res. Atmos.*, 126, e2021JD034814. doi:10.1029/2021JD034814

Bukowski, J., & van den Heever, S. C. (2022). The impact of land surface properties on haboobs and dust lofting. *J. Atmos. Sci.*, 79, 3195–3218. doi:10.1175/JAS-D-22-0001.1

Bukowski, J., & van den Heever, S. (2023). Data from: The impact of land surface properties on haboobs and dust lofting [Dataset]. Dryad. https://doi.org/10.5061/dryad.6hdr7sr4d

Byers, H. R., & Braham Jr., R. R. (1949). *The Thunderstorm*. U.S. Govt. Printing Office, 287 pp.

Chils, J., & Delfiner, P. (1999). Geostatistics: Modeling spatial uncertainty. *John Wiley Sons, Inc.* doi:10.1002/9780470316993

Cotton, W. R., Pielke, R. A., Walko, R. L., Liston, G. E., Tremback, C. J., Jiang, H., et al. (2003). RAMS 2001: Current status and future directions. *Meteorology and Atmospheric Physics*, 82(1-4), 5-29. https://doi.org/10.1007/s00703-001-0584-9

Dipankar, A., Stevens, B., Heinze, R., Moseley, C., Zängl, G., Giorgetta, M., & Brdar, S. (2015). Large eddy simulation using the general circulation model ICON. *J. Adv. Model. Earth Sy.,* 7, 963-986. doi:10.1002/2015MS000431

Droegemeier, K., & Wilhelmson, R. (1987). Numerical simulation of thunderstorm outflow dynamics. Part I: Outflow sensitivity experiments and turbulence dynamics. *Journal of the Atmospheric Sciences*, 44(8), 1180–1210. https://doi.org/10.1175/1520-0469(1987)044<1180:NSOTOD>2.0CO;2

Engerer, N. A., Stensrud, D. J., & Coniglio, M. C. (2008). Surface Characteristics of Observed Cold Pools. *Monthly Weather Review*, *136*(12), 4839–4849. https://doi.org/10.1175/2008MWR2528.1

Falk, N. M., Grant, L. D., & van den Heever, S. C. (2023). Code for CS-TropOce Simulations (v2.0.0) [Dataset]. Zenodo. https://doi.org/10.5281/zenodo.8411499

Feng, Z., Hagos, S., Rowe, A. K., Burleyson, C. D., Martini, M. N., & de Szoeke, S. P. (2015). Mechanisms of convective cloud organization by cold pools over tropical warm ocean during the AMIE/DYNAMO field campaign. *Journal of Advances in Modeling Earth Systems*, 7(2), 357–381. https://doi.org/10.1002/2014MS000384

Fiévet, R., Meyer, B., & Haerter, J. O. (2023). On the sensitivity of convective cold pools to mesh resolution. *Journal of Advances in Modeling Earth Systems*, 15, e2022MS003382. https://doi.org/10.1029/2022MS003382

Fujita, T.T. (1978). *Manual of downburst identification for project NIMROD.* University of Chicago, 104 pp.

Gentine, P., Garelli, A., Park, S.-B., Nie, J., Torri, G. and Kuang, Z. (2016). Role of surface heat fluxes underneath cold pools. *Geophys. Res. Lett.*, 43, 874–883. https://doi.org/10.1002/2015GL067262

Grant, L. D., & van den Heever, S. C. (2016). Cold pool dissipation. *Journal of Geophysical Research: Atmospheres*, 121(3), 1138–1155. https://doi.org/10.1002/2015jd023813

Grant, L. D., & van den Heever, S. C. (2018a). Cold pool-land surface interactions in a dry continental environment. *J. Adv. Model. Earth Sy.,* 10, 1513–1526. doi: 10.1029/2018MS001323

Grant, L. D., & van den Heever, S. C. (2018b). RAMS model simulation output for "Cold pool - land surface interactions in a dry continental environment" [Dataset]. Mountain Scholar. doi: 10.25675/10217/186403

Hardy, K. R., & Ottersten, H. (1969). Radar investigations of convective patterns in the clear atmosphere. *J. Atmos. Sci.*, 26, 666–672. doi:10.1175/1520-0469(1969)26,666:RIOCPI.2.0.CO;2

Hirt, M., Craig, G. C., Schäfer, S. A. K., Savre, J., & Heinze, R. (2020). Cold pool driven convective initiation: using causal graph analysis to determine what convection permitting models are missing. Quarterly Journal of the Royal Meteorological Society. https://doi.org/10.1002/qj.3788

Hohenegger, C., Ament, F., Beyrich, F., Löhnert, U., Rust, H., Bange, J., et al. (2023). FESSTVaL: the Field Experiment on Submesoscale Spatio-Temporal Variability in Lindenberg. *Bull. Am. Meteorol. Soc.* doi:10.1175/BAMS-D-21-0330.1

Huang, Q., Marsham, J. H., Tian, W., Parker, D. J., & Garcia-Carreras, L. (2018). Large-eddy simulation of dust-uplift by a haboob density current. *Atmos. Environ.*, 179, 31–39. doi:10.1016/j.atmosenv.2018.01.048

Khairoutdinov, M., & Randall, D. (2006). High-resolution simulation of shallow-to-deep convection transition over land. *Journal of the Atmospheric Sciences*, 63(12), 3421–3436. https://doi.org/10.1175/JAS3810.1

Kirsch, B., Ament, F., & Hohenegger, C. (2021). Convective Cold Pools in Long-Term Boundary Layer Mast Observations. *Mon. Wea. Rev.*, 149, 811–820, doi:10.1175/MWR-D-20-0197.1

Kirsch, B., Hohenegger, C., Klocke, D., & Ament, F. (2022a). Meteorological network observations by APOLLO and WXT weather stations during FESSTVaL 2021 (Version 00-2) [Dataset]. Integrated Climate Data Center, Universität Hamburg. doi:10.25592/uhhfdm.10179

Kirsch, B., Hohenegger, C., Klocke, D., Senke, R., Offermann, M. & Ament, F. (2022b). Sub-mesoscale observations of convective cold pools with a dense station network in Hamburg, Germany. *Earth Syst. Sci. Data*, 14, 3531–3548. doi:10.5194/ESSD-14-3531-2022

Kirsch, B., Hohenegger, C., & Ament, F. (2023a). Morphology and growth of convective cold pools observed by a dense station network in Germany. *Q. J. Roy. Meteor. Soc.* (accepted pending revisions).

Kirsch, B., Grant, L. D., Bukowski, J., Falk, N. M. & Neumaier, C. A. (2023b). How-variable-are-cold-pools_Grant-etal (Version v1.0-submitted) [Dataset]. Zenodo. https://doi.org/10.5281/8433896

Lord Rayleigh O.M. F.R.S. (1916). LIX. On convection currents in a horizontal layer of fluid, when the higher temperature is on the under side. *The London, Edinburgh, and Dublin Philosophical Magazine and Journal of Science*, 32:192, 529-546. doi:10.1080/14786441608635602

Marks, G. B., Colquhoun, J. R., Girgis, S. T., Koski, M. H., Treloar, A. B. A., Hansen, P., et al. (2001). Thunderstorm outflows preceding epidemics of asthma during spring and summer. *Thorax*, 56(6), 468–471. https://doi.org/10.1136/thx.56.6.468

Neumaier, C. A. , Grant, L. D., & van den Heever, S. C. (2023). Code for IDEAL-Shear Simulations (v1.1.0) [Dataset]. Zenodo. https://doi.org/10.5281/zenodo.8411979

Purdom, J. F. W. (1976). Some uses of high-resolution GOES imagery in the mesoscale forecasting of convection and its behavior. Monthly Weather Review, 104(12), 1474–1483. https://doi.org/10.1175/1520-0493(1976)104<1474:SUOHRG>2.0.CO;2

Reid, J. S., Maring, H. B., Narisma, G. T., van den Heever, S. C., DiGirolamo, L., Ferrare, R. et al. (2023). The coupling between tropical meteorology, aerosol science, convection and the energy budget during the Clouds, Aerosol Monsoon Processes Philippines

Experiment (CAMP2Ex). *Bull. Amer. Met. Soc.*, 104, E1179-E1209. https://doi.org/10.1175/BAMS-D-21-0285.1

Rotunno, R., Klemp, J. B., & Weisman, M. L. (1988). A theory for strong, long-lived squall lines. *Journal of the Atmospheric Sciences*, 45(3), 463–485. https://doi.org/10.1175/1520-0469(1988)045<0463:ATFSLL>2.0.CO;2

Sakradzija, M. (2023). ICON-LES for FESSTVaL: Jogi cold pool 2021-06-29 (Version v1) [Dataset]. Zenodo. https://doi.org/10.5281/zenodo.8411098

Saleeby, S. M., & van den Heever, S. C. (2013). Developments in the CSU-RAMS Aerosol Model: Emissions, Nucleation, Regeneration, Deposition, and Radiation. *J. Appl. Meteor. Climatol.*, **52**, 2601–2622, https://doi.org/10.1175/JAMC-D-12-0312.1

Schlemmer, L., & Hohenegger, C. (2014). The formation of wider and deeper clouds as a result of cold-pool dynamics. *Journal of the Atmospheric Sciences*, 71(8), 2842–2858. https://doi.org/10.1175/JAS-D-13-0170.1

Seigel, R. B., and van den Heever, S. C. (2012). Dust Lofting and Ingestion by Supercell Storms. *J. Atmos. Sci.*, **69**, 1453–1473. https://doi.org/10.1175/JAS-D-11-0222.1

Simoes-Sousa, I. T., Tandon, A., Buckley, J., Sengupta, D., Sree, L. J., Shroyer, E., & de Szoeke, S. P. (2022). Atmospheric Cold Pools in the Bay of Bengal. *Journal of the Atmospheric Sciences*, *80*(1), 167–180. https://doi.org/10.1175/JAS-D-22-0041.1

Simpson, J. E. (1969.) A comparison between laboratory and atmospheric density currents. *Q. J. Roy.Meteor. Soc.*, 95, 758–765. https://doi.org/10.1002/qj.49709540609

Straka, J. M., Wilhelmson, R. B., Wicker, L. J., Anderson, J. R., & Droegemeier, K. K. (1993). Numerical solutions of a non-linear density current: A benchmark solution and comparisons. *International Journal for Numerical Methods in Fluids*, 17(1), 1–22. https://doi.org/10.1002/fld.1650170103

Terai, C. R. and Wood, R. (2013). Aircraft observations of cold pools under marine stratocumulus. *Atmos. Chem. Phys.*, 13, 9899–9914. https://doi.org/10.5194/ACP-13-9899-2013

van den Heever, S. C., Grant, L. D., Freeman, S. W., Marinescu, P. J., Barnum, J., Bukowski, J., et al. (2021). The Colorado State University Convective CLoud Outflows and UpDrafts Experiment (C3LOUD-Ex). *Bull. Am. Meteorol. Soc.*, 102, E1283–E1305. doi:10.1175/BAMS-D-19-0013.1

Wackernagel, H. (2003). Multivariate geostatistics: An introduction with applications. *Springer*, 3rd edition.

Wilson, J. W., & Schreiber, W. E. (1986). Initiation of convective storms at radar-observed boundary-layer convergence lines. *Monthly Weather Review*, 114(12), 2516–2536. https://doi.org/10.1175/1520-0493(1986)114<2516:IOCSAR>2.0.CO;2

Zuidema, P., Li, Z., Hill, R. J., Bariteau, L., Rilling, B., Fairall, C., et al. (2012). On Trade Wind Cumulus Cold Pools. *Journal of the Atmospheric Sciences*, *69*(1), 258–280. https://doi.org/10.1175/JAS-D-11-0143.1

References in the Supporting Information

Feranec, J., Soukup, T., Hazeu, G., & Jaffrain, G. (Eds.) (2016). European landscape dynamics. Corine land cover data, CRC-Press, Boca Raton, pp. 9-14.

Harrington, J. Y. (1997). The effects of radiative and microphysical processes on simulated warm and transition season Arctic stratus. Ph.D. dissertation, Colorado State University, 301 pp.

Heinze, R., Dipankar, A., Henken, C. C., Moseley, C., Sourdeval, O., Trömel, S., et al. (2017). Large-eddy simulations over Germany using ICON: A comprehensive evaluation. *Quarterly Journal of the Royal Meteorological Society*, 143(702), 69–100. https://doi.org/10.1002/qj.2947

Hill, G. E. (1974) Factors controlling the size and spacing of cumulus clouds as revealed by numerical experiments. *J. Atmos. Sci.*, 31, 646–673. https://doi.org/10.1175/1520-0469(1974)031<0646:FCTSAS>2.0.CO;2

Lilly, D. K. (1962). On the numerical simulation of buoyant convection. *Tellus*, 14(2), 148–172. doi:10.1111/J.2153-3490.1962.TB00128.x

NASA/METI/AIST/Japan Spacesystems and U.S./Japan ASTER Science Team. ASTER Global Digital Elevation Model V003 (2019). distributed by NASA EOSDIS Land Processes Distributed Active Archive Center. Accessed 2023-10-05. https://doi.org/10.5067/ASTER/ASTGTM.003

Schulz, J.-P., & Vogel, G. (2020). Improving the processes in the land surface scheme TERRA: Bare soil evaporation and skin temperature. *Atmosphere*, 11(5), 513. doi:10.3390/atmos11050513

Smagorinsky, J. (1963). General circulation experiments with the primitive equations. *Monthly Weather Review*, 91(3), 99–164. https://doi.org/10.1175/1520-0493(1963)091<0099:GCEWTP>2.3.CO;2

Walko, R. L., Band, L. E., Baron, J., Kittel, T. G. F., Lammers, R., Lee, T. J., et al. (2000). Coupled atmosphere–biophysics–hydrology models for environmental modeling. *Journal of Applied Meteorology*, 39(6), 931–944. https://doi.org/10.1175/1520-0450(2000)039<0931:CABHMF>2.0.CO;2